

T. Jesionowski  
K. Bula  
J. Jurga  
A. Krysztafkiewicz

## Effect of amorphous precipitated silica on the properties and structure of poly(*p*-phenylene sulfide)

Received: 7 November 2000  
Accepted: 5 April 2001

T. Jesionowski (✉) · A. Krysztafkiewicz  
Institute of Chemical  
Technology and Engineering  
Poznan University of Technology  
pl. M. Skłodowskiej-Curie 2  
60-965 Poznan, Poland  
e-mail: teofil.jesionowski@put.poznan.pl  
Tel.: +48-61-6653626  
Fax: +48-61-6653649

K. Bula · J. Jurga  
Institute of Material Technology  
Poznan University of Technology  
ul. Piotrowo 3, 61-138 Poznan, Poland

**Abstract** Using a precipitation technique, silicas were obtained from sodium metasilicate solution employing an acidic agent. Alcohol solutions were used in the process of production of highly dispersed silicas, which resulted in partial blocking of the silica surface silanol groups. Moreover, studies on morphology and microstructure using transmission electron microscopy and scanning electron microscopy were performed. The size distributions of primary particles and aggregate and agglomerate structures were determined using a Zeta-Plus instrument using the dynamic light scattering method. The structure and molecular dynamics of

the nanocomposite, consisting of poly (*p*-phenylene sulfide) (PPS) and of the precipitated silica, were studied using atomic force microscopy and nuclear magnetic resonance. It was proved that during annealing the fragmentation of PPS agglomerates takes place. This phenomena probably resulted from repulsion forces existing between agglomerates and aggregates. Fragmentation in the polymer network probably resulted from repulsion forces between agglomerates and smaller aggregates.

**Key words** Amorphous silica · Composite of poly(*p*-phenylene sulfide) · Molecular structure

### Introduction

In the recent two decades, the production of polymer composites drew particular attention and included the introduction to systems of various polymers of glass fibers and carbon, minerals, carbon, graphite, soot and other fillers [1, 2, 3, 4, 5]. The technologies proved successful and the contemporary market of plastics features an entire spectrum of composite materials of high strength parameters [6, 7, 8].

Compared to conventional composite materials, the problems of polymer composite production have recently gained new dimensions owing to the introduction to polymers of nanometric-sized inorganic particles which promote changes in physical and chemical interactions between the dispersed phase [9, 10, 11]. The introduction of the dispersed silica particles to a polymer template provides access to the so-called subtle polymer structure.

The potential stems from a distinct type of the interactions, their distinct scope and the chance of manipulating the composite structure at the level of a molecule [11]. The application of semicrystalline poly(*p*-phenylene sulfide) (PPS) is connected with a specific crystalline structure of this material. Processed parts of the unfilled PPS, injected into the hot mold, contain a high number of pores despite extensive degassing of the plastic before its processing. Studies employing atomic force microscopy (AFM) permit observation of the PPS structure on a nanometer scale and have proven that the crystalline structure of PPS contains defects and discontinuities. This results in a reduction in the mechanical properties and in a more pronounced crystalline character of the polymer. Taking advantage of the natural defects in the polymer structure and its probably extensive active surface the attempt should be made to fill the defects in the PPS structure by the introduction to

the polymer of a nanometric silica dispersion with the size of its particles corresponding to the dimensions of the defects. Keeping this in mind, studies were undertaken to obtain highly dispersed silicas of nanometric particles by precipitation from sodium metasilicate solution [12, 13].

## Experimental

### Method of precipitating highly dispersed nanometric silica

Highly dispersed silicas were obtained by precipitation from a solution of sodium metasilicate,  $\text{Na}_2\text{O} \cdot m\text{SiO}_2 \cdot n\text{H}_2\text{O}$ , using diluted acids (hydrochloric acid, sulfuric acid) or an acid anhydride (technical  $\text{CO}_2$ ) in an alcohol medium.

For the production of the hydrated silicas, 5% sodium metasilicate solution, with a silicate modulus of 3.3, and 2-propanol, ethylene glycol or glycerin were used. In the precipitation process, basic factors which affected the physicochemical parameters of the product obtained were determined. The results permitted optimization of the conditions of the hydrated silica precipitation.

The process of precipitating silica from sodium metasilicate solution in the presence of an acid or acid anhydride is presented graphically in Fig. 1.

In the first stage, an appropriate alcohol was introduced to the reactor. Using a peristaltic pump, sodium metasilicate solution and the acid were dosed at a constant rate into the reactive mixture.

Alternatively, the process of precipitating highly dispersed silica was performed using gaseous  $\text{CO}_2$ . The reaction was performed at a temperature slightly lower than the boiling point of the organic solvent. Following the precipitation reaction, the pH of the system was corrected using a diluted acid (hydrochloric or sulfuric). The resulting sediment was dried and deagglomerated in an electric mortar (Fritsch Pulverisette, Germany).

The principal parameters in obtaining highly dispersed silicas in the presence of various alcohols are presented in Table 1.

The highly dispersed silicas were subjected to physicochemical, structural, and microscopic appraisal, and their surface properties were tested. Basic physicochemical tests were performed as described earlier [14, 15]. The particle size distribution and the zeta potential were measured using a ZetaPlus apparatus (Brookhaven Instruments, USA) by the dynamic and electrophoretic light scattering techniques.

In order to obtain data on the morphology of the particles, the structure of individual particles and the agglomerates, transmission electron microscopy (single-stage replica technique) and scanning electron microscopy were performed, using JEM 1200 EX2 and Phillips SEM 515 electron microscopes.

### Preparation of PPS composites

Pristine PPS (RYTON PPS V-1) from Phillips Petroleum Company and composites made of RYTON PPS V-1 and synthesized  $\text{SiO}_2$  (obtained in the ethylene glycol medium) were applied. In such conditions the  $\text{SiO}_2$  particle size was compatible with the dimensions of interagglomerate free volume of virgin PPS [16]. After 10-h drying in a vacuum at 105 and 120 °C for silica and PPS, respectively, the powdered components were weighed separately according to the desired silica content of 20% by dry weight and mixed together in a rotating container. The container was equipped with parallel mixing elements and the rotation speed was 50 rpm. Injection molding was performed in the cold mold (at 50 °C) with

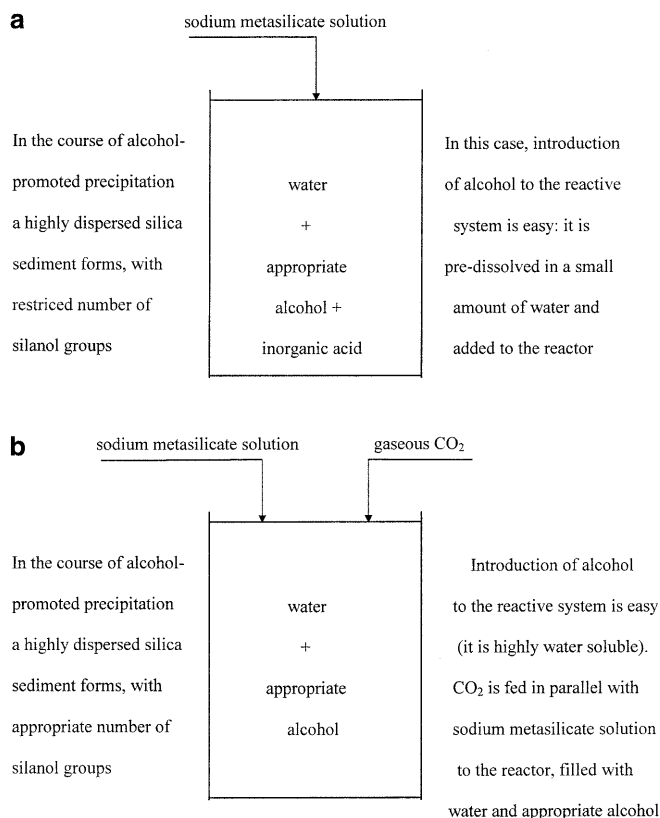


**Fig. 1a,b** The process of precipitation of highly dispersed silica from sodium metasilicate. **a** The case of using mineral acid to precipitate silica; **b** the case of using gaseous  $\text{CO}_2$  to precipitate silica

an ENGEL ES 80/20 HLS machine for PPS and its composites. Injection molding at higher temperatures (above 80 °C) is not possible with used injection mold part of the ENGEL machine. The samples prepared for testing were divided into two groups. The first group of the samples was subjected to AFM and NMR investigations. The remaining ones were annealed at 150 °C for 1 h and then tested by the same techniques. For comparison of the results, injection-molded pristine PPS samples were also investigated.

Scanning transmission microscopy (STM)/AFM (OMICRON) equipment was been used at room temperature to study the topography of the polymer and its composite. Atomic force microscope images obtained with constant force mode were applied. For AFM observation the sample was placed on a single-tube piezoelectric translator by using the tips of silicon nitride ( $\text{Si}_3\text{N}_4$ ) fixed under a cantilever. The maximum area available to scan was  $5000 \times 5000 \text{ nm}^2$  and typical images consisted of  $256 \times 256$  dots/line. The scanning rate was within the range of a few hertz per line. The STM/AFM resolution was 0.01 nm in the  $z$  direction and 0.05 nm on the surface plane.

Temperature spin-lattice relaxation time measurements for PPS/ $\text{SiO}_2$  composites were carried out with a pulse NMR spectrometer, operating at 30 MHz for protons [17]. The measurements were performed within the temperature range from -100 to 10 °C. The sample temperature was maintained by blowing liquid nitrogen. The relaxation times,  $T_1$ , were measured by means of  $\pi/2 - \tau - \pi/2$ , according to the conventional method. The duration of the  $\pi/2$  pulse was 2  $\mu\text{s}$  and the dead time of the spectrometer was 10  $\mu\text{s}$ .

**Table 1** Parameters of precipitating highly dispersed silicas using an appropriate alcohol as a modifying agent

Sample number	Parameters of obtaining highly dispersed silicas	Observation and remarks
2-Propanol 1	$T = 80\text{ }^{\circ}\text{C}$  5% solution of sodium metasilicate 5% $\text{H}_2\text{SO}_4$ solution 2-Propanol: $\text{Na}_2\text{O} \cdot \text{SiO}_2$ : $\text{H}_2\text{SO}_4 = 1:2:0.5$ pH 1	A gel-like sediment of coarse granules, poorly filterable, was obtained
Ethylene glycol 2	$T = 85\text{ }^{\circ}\text{C}$  5% solution of sodium metasilicate 0.8% glycol solution Ethylene glycol: $\text{Na}_2\text{O} \cdot \text{SiO}_2$ : $\text{H}_2\text{SO}_4 = 1:2:2.5$ pH 4	A very well dispersed sediment was obtained
Glycerin 3	$T = 85\text{ }^{\circ}\text{C}$  5% solution of sodium metasilicate 0.8% glycerin solution $\text{CO}_2$ – flow rate – $15\text{ dm}^3/\text{hdm}^3$ Glycerin: $\text{Na}_2\text{O} \cdot \text{SiO}_2 = 1:2$ pH 6	A very well dispersed sediment was obtained

## Results and discussion

Basic physicochemical parameters such as bulk density, water and paraffin oil absorbing capacities, aggregate size distribution and the electrokinetic (zeta) potential of the silicas obtained are presented in Table 2.

The hydrated silicas obtained demonstrated variable physicochemical parameters. The most extensively dispersed silicas were obtained upon precipitation in the presence of ethylene glycol or glycerin. The silicas manifested a very high paraffin oil absorbing capacity ( $1300\text{--}1500\text{ cm}^3/100\text{ g}$ ) and a low bulk density ( $63\text{--}95\text{ g/dm}^3$ ).

The agglomerate size distributions of the silica precipitated in the three alcohols are shown in Figs. 2, 3, 4. The hydrated silica, precipitated in the 2-propanol contained agglomerates of a relatively large diameter (of order  $525\text{ nm}$ ) and showed a tendency to form agglomerates approximately  $1340\text{ nm}$  in diameter. Precipitation of the hydrated silica in the presence of polyhydroxyl alcohols resulted in the formation of significantly smaller agglomerates of particles (diameter around  $112\text{ nm}$  in glycerin

and around  $360\text{ nm}$  in ethylene glycol – Figs. 3, 4). The results of the studies on the particle size distribution were confirmed by microscopic observations.

The formation of large agglomerates of variable shape and size in the presence of the organic agent 2-propanol is shown in Fig. 5. Silica precipitated in the medium of ethylene glycol manifested highly dispersed particles and showed an insignificant fraction of aggregates and agglomerates (Fig. 6). On the other hand, the hydrated silica obtained in glycerin showed very fine particles and a still lower tendency to form aggregates and agglomerates compared to the alcohols mentioned earlier. The latter silica tended to form spherical structures, consisting of fine particles (Fig. 7).

In contrast to products obtained in the presence of monohydroxyl alcohols, silicas precipitated in ethylene glycol and glycerin exhibited an extensively developed outer surface.

The results of AFM studies in constant force mode of injection-molded PPS/ $\text{SiO}_2$  composites are presented in Figs. 8 and 9. Extremely different results for those of pristine PPS and its composites have been detected.

**Table 2** Physicochemical parameters of the precipitated silicas obtained

Sample number	Paraffin oil absorbing capacity ( $\text{cm}^3/100\text{ g}$ )	Water absorbing capacity ( $\text{cm}^3/100\text{ g}$ )	Bulk density ( $\text{g/dm}^3$ )	Mean size of agglomerates (nm)	Zeta potential (mV)
1	450	150	293.1	651.0	-67.1
2	1,300	450	95.0	846.0	-27.5
3	1,500	500	63.0	760.0	-19.8

Below the glass-transition temperature of PPS ( $T_g = 92^\circ\text{C}$ ) for samples molded at  $50^\circ\text{C}$  the crystallinity

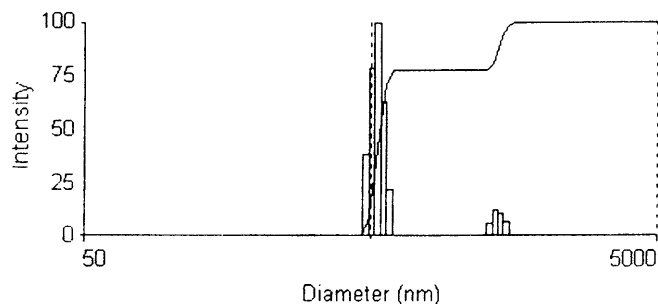


**Fig. 2** Particle size distributions of silica obtained in 2-propanol

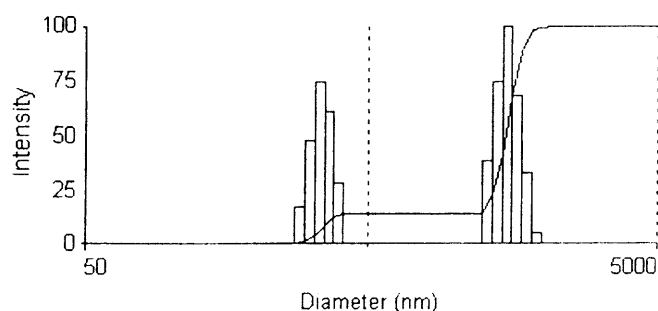


**Fig. 3** Particle size distributions of silica obtained in ethylene glycol

is very low (amorphous) [16, 17, 18, 19, 20]. The AFM image of amorphous PPS shows very long agglomerates with an average width of around 100 nm (Fig. 8a). Heat treatment at  $150^\circ\text{C}$  for 1 h increased the crystallinity of PPS and simultaneously broke down the long agglomerates to small aggregates [16] which still remained connected with very narrow bands (Fig. 8b).

Between aggregates 8-nm deep holes have been observed. The average diameter of the aggregates is about 150 nm and the height is approximately 8 nm. The width of the bands is about 20 nm (Fig. 8b).

The AFM data collected for PPS/SiO<sub>2</sub> composites, presented in Fig. 9a, document much larger agglomerates compared to the unfilled PPS. The average diameter of these agglomerates is 800 nm. Annealing at  $150^\circ\text{C}$  for 1 h was also applied to this composite. The change in

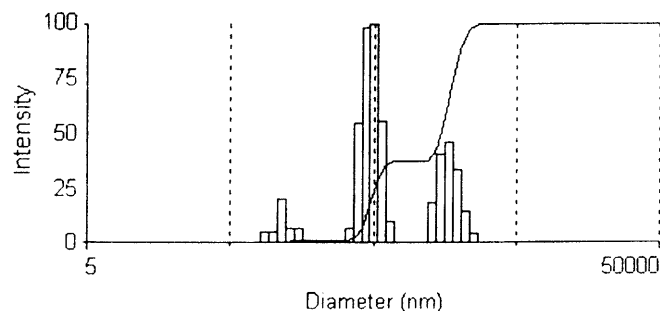


**Fig. 4** Particle size distributions of silica obtained in glycerin

**Fig. 5** Micrographs of precipitated silicas in 2-propanol: **a** transmission electron microscopy (20,000 $\times$ ); **b** scanning microscopy (2,500 $\times$ )

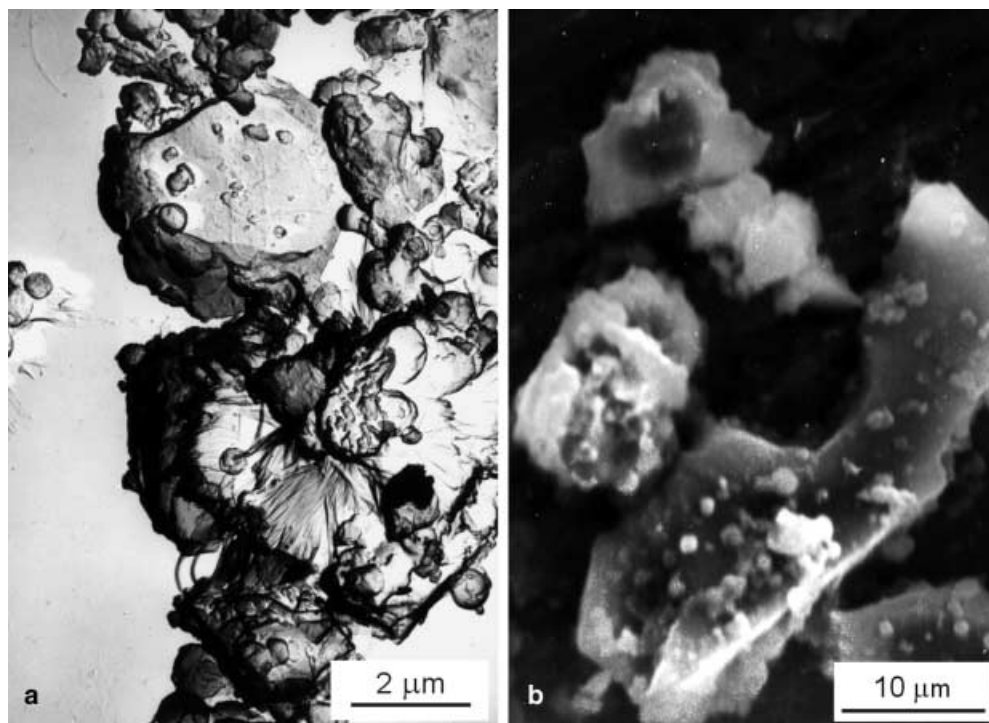


**Fig. 6** Micrographs of silicas precipitated in ethylene glycol: **a** transmission electron microscopy (20,000 $\times$ ); **b** scanning microscopy (2,500 $\times$ )

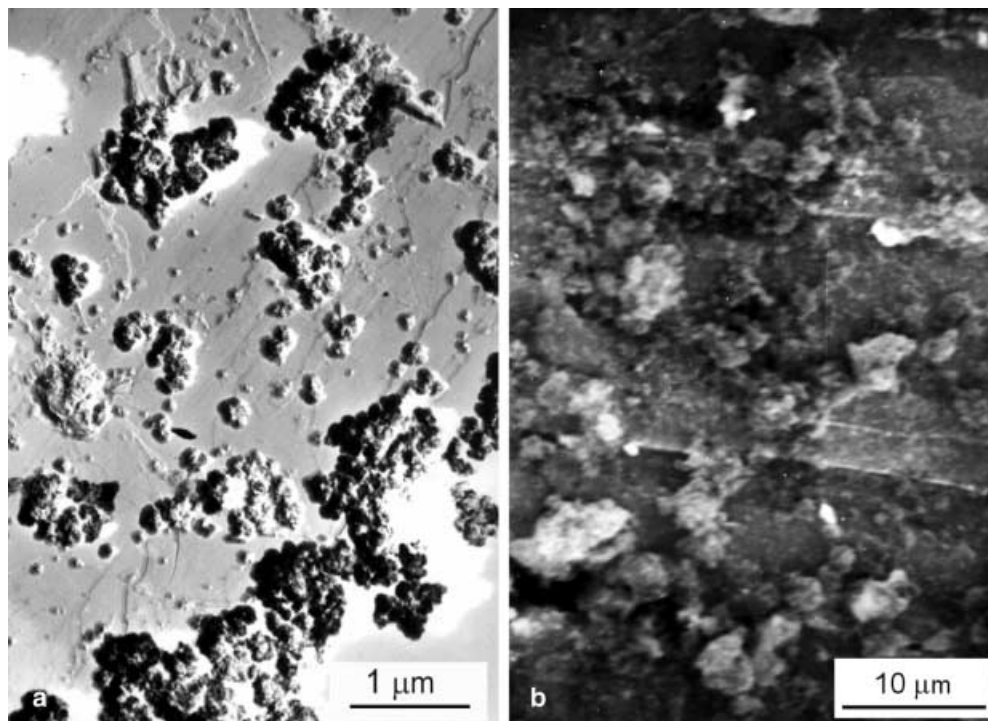
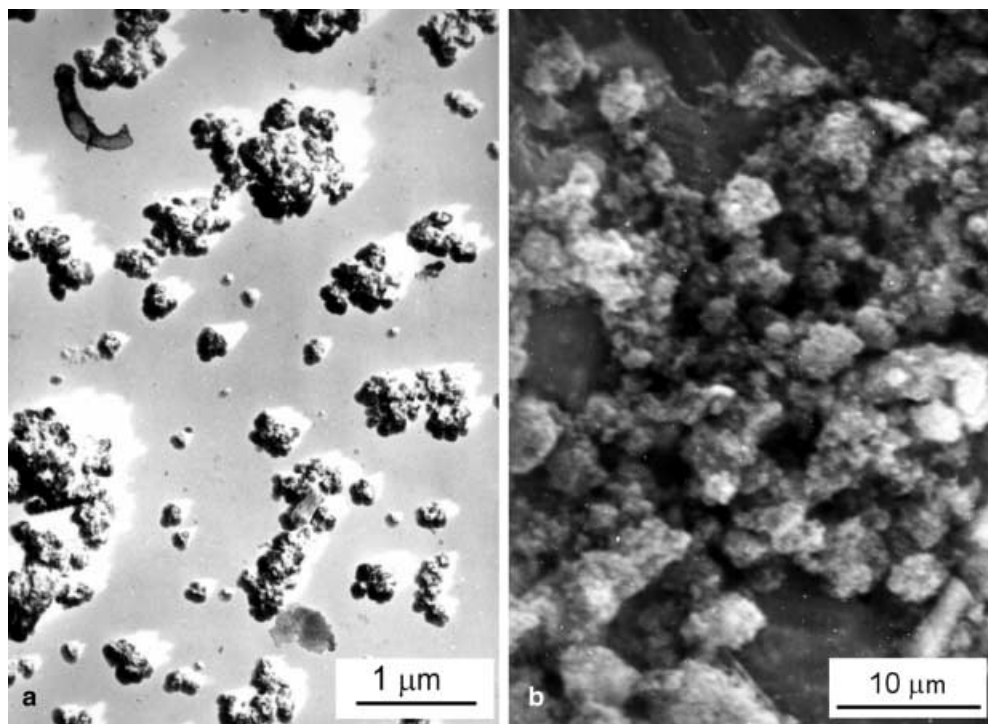


**Fig. 7** Micrographs of silicas precipitated in glycerin: **a** transmission electron microscopy (20,000 $\times$ ); **b** scanning microscopy (2,500 $\times$ )



the surface morphology was observed in the same manner as observed in pristine PPS (Fig. 8b). After annealing, the PPS/SiO<sub>2</sub> composites were twice as large as PPS without filler (Fig. 9b).

The temperature proton spin-lattice relaxation time dependences in the case of PPS and its composites with SiO<sub>2</sub> after injection and heat treatment (annealing) are presented in Fig. 10. The temperature dependence of

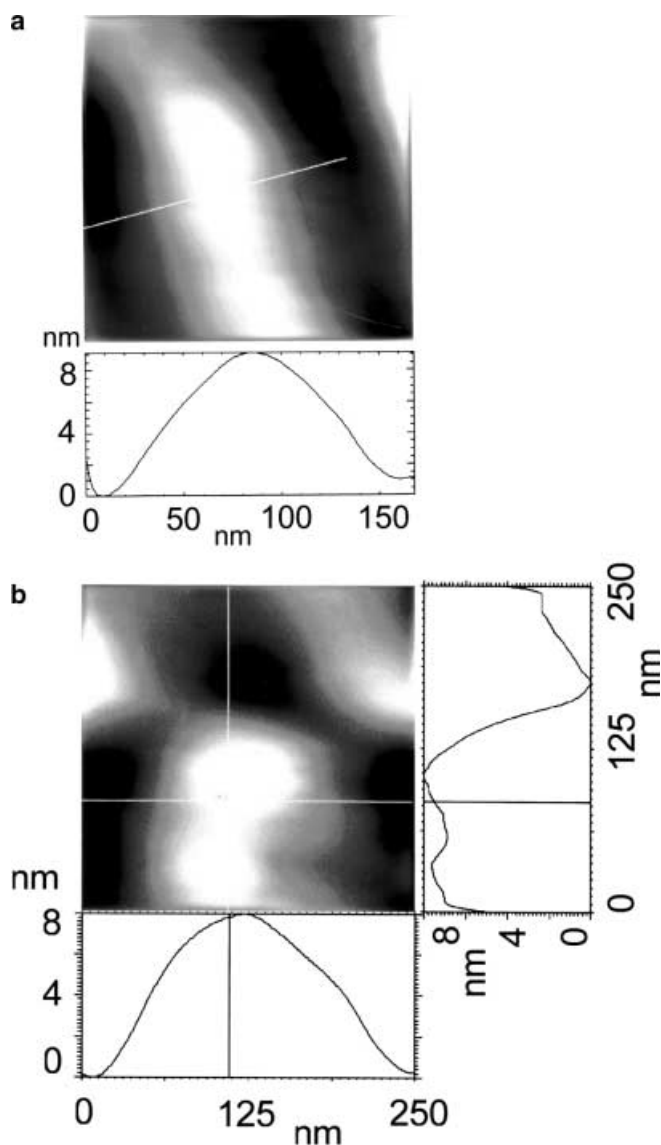


**Fig. 8** Atomic force microscopy (AFM) image of pristine poly(*p*-phenylene sulfide) (PPS) **a** injected into the cold mold (50 °C), **b** annealed at 150 °C after injection into the cold mold

relaxation time  $T_1$  of unfilled PPS is similar to that discovered earlier in commercial grades of RYTON PPS R-4 and PPS R-6 obtained after annealing [18]. In both cases the recoveries of the magnetization were exponential. The introduction of mineral filler to pristine PPS changed the recovery of the magnetization in a nonexponential manner. In the case of PPS composites, the temperature dependence of the relaxation time shows a very sharp increase followed by a minimum.

The surface morphology of pristine PPS and its composites was interpreted as an interfacial strain effect in the polymer network. The polymer probably con-

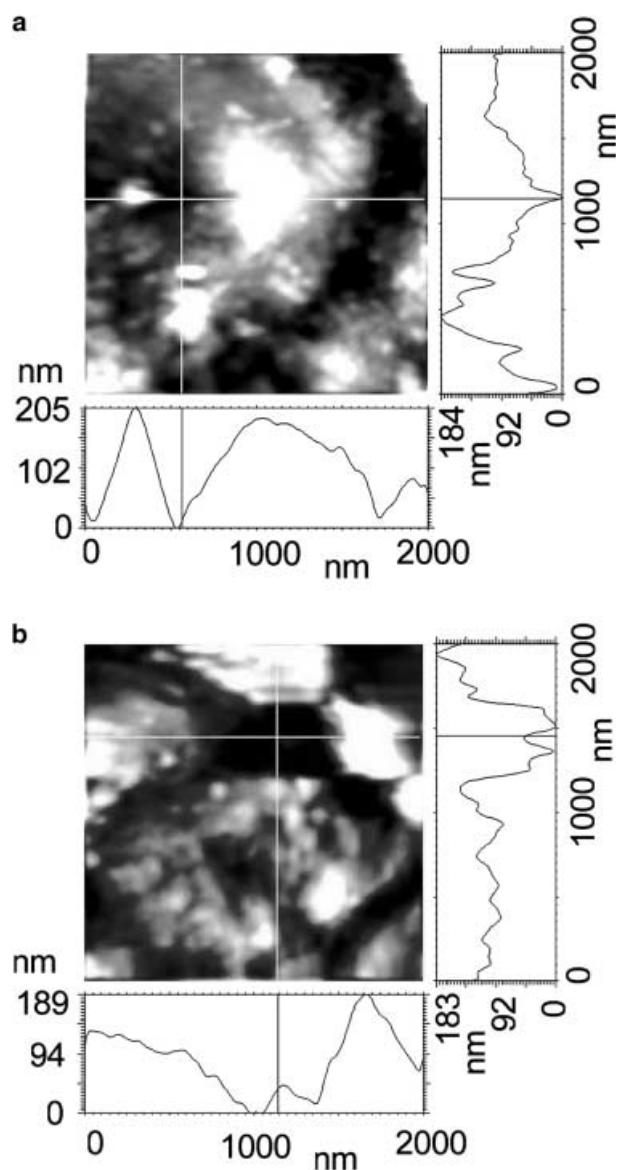


**Fig. 9** AFM image of PPS/SiO<sub>2</sub> composite **a** injected into the cold mold, **b** annealed at 150 °C after injection into the cold mold

tained fragments of its morphological structure in which internal stress took place. Therefore, it is suggested that the introduction of SiO<sub>2</sub> filler to the polymer network increased the distance between aggregates. This led to a limited exchange in energy of protons between the neighboring aggregates. The distances between agglomerates and aggregates are substantial compared with the distance in which dipolar interactions take place. For this reason it is assumed that nonexponential recoveries of the magnetization in mineral-filled PPS are connected with the interaction between nuclear spins inside some particles. Thus, the nature of the interactions between aggregate or agglomerate systems differs from the

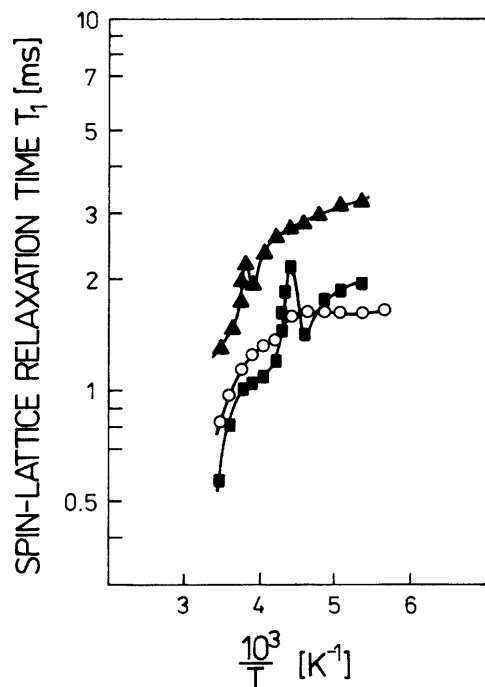


**Fig. 10** Temperature dependence of spin-lattice relaxation time  $T_1$  for pristine PPS (○), PPS/SiO<sub>2</sub> composite without annealing (■), PPS/SiO<sub>2</sub> composite annealed at 150 °C for 1 h (▲)

interaction inside them. It is assumed that these systems interact owing to electrostatic charges located on the polymer chains, which cause mutual repulsion. Paramagnetic centers in this polymer located on the main chain of the polymer and oligomers represent the probable source of these interactions [19, 20]. The

centers were also observed in injection molding of pristine PPS by electron paramagnetic resonance [20].

## Conclusions

- The silicas obtained in the process of precipitation from sodium metasilicate solutions in the presence of ethylene glycol or glycerin exhibit features which permit their broad application, for example, in processing of PPS.
- The exponential recovery of the magnetization for pristine PPS suggests that the exchange of spin energy between aggregates is rapid as a result of good contact between different phases of the polymer. The introduction of a filler to the polymer changes the interaction mechanism. Inside the agglomerates and also the aggregates a dipole–dipole interaction mechanism operates. This interaction is opposite to the electrostatic interaction between these systems. The contact between different composite polymer phases is weak and therefore a nonexponential recovery of the magnetization is observed. This seems to indicate that the molecular reorientation of protons is independent in each of the phases.
- AFM and NMR studies of unfilled and mineral-filled PPS show that fragmentation during annealing in both cases has the same nature. Repulsion forces operate between agglomerates and smaller aggregates are probably the source of fragmentation in the polymer network.

**Acknowledgements** This work was partially supported by research grant nos. DPB 62–169 and DS 32/008/2000.

## References

1. Ou Y, Yang F, Zhong-Zhen Y (1998) *J Polym Sci Part B Polym Phys* 36:789
2. Zhou W, Dong H, Qui Y, Wei Y (1998) *J Polym Sci. Part A Polym Chem* 36:1607
3. David A, Siuzdak D, Kenneth A, Mauritz K (1999) *J Polym Sci Part B Polym Chem* 37:143
4. Jiang S, Yu D, Ji X, An L, Jianh B (1999) *Polymer* 41:2041
5. Brady D. G (1976) *J Appl Polym Sci* 20:2541
6. Krysztafkiewicz A, Jesionowski T, Rager B (1997) *J Adhes Sci Technol* 11:507
7. Krysztafkiewicz A, Maik M, Rager B (1992) *J Mater Sci* 27:3581
8. Krysztafkiewicz A, Maik M, Rager B (1993) *Powder Technol* 75:29
9. Kraus G. (1965) *Reinforcement of elastomers*. Interscience, New York
10. Wolff S (1988) *Kautsch Gummi Kunstst* 41:674
11. Krysztafkiewicz A (1989) *Colloid Polym Sci* 267:399
12. Jesionowski T, Krysztafkiewicz A (2000) *J Non-Cryst Solids* 277:45
13. Krysztafkiewicz A, Jesionowski T, Binkowski S (2000) *Colloids Surf A* 173:73
14. Krysztafkiewicz A (1987) *Chem Stosow* 31:443
15. Jesionowski T, Krysztafkiewicz A (1999) *J Dispersion Sci Technol* 20:1609
16. Jurga J, Garbarczyk J, Susla B, Czajka R, Ciesielska D (1997) 2Tu7 *Proceedings of the 1st International Symposium on Scanning Probe Spectroscopy and Related Methods*
17. Jurga J, Jurga K (1989) *Sci Instrum* 2:23
18. Jurga J, Hruszka P (1993) *Polymer* 34:2072
19. Kreja L, Rozploch F (1988) *Makromol Chem* 160:163
20. Jurga J, Kruczynski Z, Krzyminewski R, Garbarczyk J, Bula K (2000) 38th *Macromolecular IUPAC Symposium Warsaw vol 3. IUPAC*, p 1286